Embedded TDR wire-like sensing elements for monitoring applications

Publisher version avaialble:
https://www.sciencedirect.com/science/article/pii/S0263224115001141

DOI: 10.1016/j.measurement.2015.02.050

Embedded TDR wire-like sensing elements for monitoring applications

Andrea Cataldo[a], Egidio De Benedetto[a], Giuseppe Cannazza[a], Emanuele Piuzzi[b], Nicola Giaquinto[c]

[a]*Department of Engineering for Innovation - University of Salento, Complesso Ecotekne - Corpo O, via Monteroni, 73100 Lecce, Italy, andrea.cataldo@unisalento.it*
[b]*Department of Information Engineering, Electronics and Telecommunications - Sapienza University of Rome, Via Eudossiana 18, 00184 Roma, Italy, piuzzi@diet.uniroma1.it*
[c]*Department of Electric and Information Engineering - Polytechnic of Bari, via E. Orabona 4, 70125 Bari, Italy, giaquinto@misure.poliba.it*

Abstract

The present work describes two practical application scenarios for an innovative, diffused, low-cost sensing system, which can be permanently embedded in the system to be monitored (STBM), thus allowing the continuous, real-time monitoring over its whole life cycle. The basic idea of the considered sensing system is to endow the STBM with flexible, wire-like sensing elements (SE's), to be used in conjunction with time domain reflectometry (TDR). One of the crucial advantages of the proposed sensing system is that a SE could be tens of meters long; hence, one single SE may suffice to monitor large areas in a single shot.
The two practical applications considered in this paper relate to moisture monitoring of building structures and to the management of irrigation in agriculture: for each of these application fields, preliminary experimental tests were performed, and the potential and limitations of the considered sensing system were assessed. Finally, in order to evaluate the metrological performance of the sensing systems, an additional set of experiments was carried out employing six different types of wire-like SE's and the obtained results were comparatively assessed.

Keywords: moisture measurements, irrigation, structural health monitoring, time domain reflectometry, water management

1. Introduction

Smart monitoring and diagnostics have become essential, and monitoring systems are now expected to be reliable, effective, accurate, and possibly maintenance-free. Still, monitoring systems are also required to be inexpensive. Another desired requirement is non-destructiveness, which becomes mandatory when dealing with 'structures' which must not be destroyed or altered. Some of the state-of-the-art solutions for nondestructive monitoring rely on electromagnetic methods, such as ground penetrating radar [1–3] and microwave transmission/reflection measurements [4, 5]. One of the possible technological solution to meet, simultaneously, all of the aforementioned requirements is to endow the system to be monitored (STBM) with built-in sensors, which remain permanently within the system and which can be interrogated non-invasively whenever necessary. However, most of the available embeddable sensors are local or point sensors; therefore, to monitor large areas/volumes, a high number of sensors should be employed. An addition downside is that most embeddable sensors often work on battery; hence, they require periodic maintenance.
Starting from these considerations, the present work addresses the possibility of employing low-cost, passive, flexible, wire-like sensing elements (SE's) to be used in conjunction with time domain reflectometry (TDR). Similarly to the sensing elements employed in [6–8] for the localization of water leaks in underground pipes, the

basic idea is to extend the principles of punctual TDR-based monitoring to multi-purpose networks of diffused SEs, embedded permanently within the STBM's. One of the major advantages of the proposed sensing system is that the considered SE may be tens of meters long and can follow any desired path inside the STBM, thus allowing to obtain a diffused profiling with a single SE. Furthermore, these SE's are passive; hence, they do not require maintenance. It is worth mentioning that, at the state of the art, optical fibre-based sensor technology represents a well-established solution for humidity and moisture measurements; in this regard, a number of key applications are highlighted in [9]. As a matter of fact, fiber optics has also been used to obtain the distributed measurements of water content [10]; however, although the provided measurement accuracy is high, the costs of the involved instrumentation are still quite prohibitive for massive deployment of such apparata.

In view of potential practical applications, this work investigates the feasibility of employing the proposed systems in two major application contexts: *i*) moisture monitoring of building structures, and *ii*) monitoring of soil moisture content for management of irrigation in agriculture.

With regards to the former application, most of the state-of-the-art embeddable moisture sensors are local sensors, with limited sensing volume [11–14]; therefore, numerous sensors are required to obtain an adequate spatial resolution of the moisture profile. Moreover, most of these sensors requires batteries and the sophisticated electronics may not last long inside construction materials. On the other hand, the passive wire-like SE's proposed in this paper could be inserted inside building structures, following the desired path, thus allowing to obtain a diffused monitoring system of the structure in use (*ex-post monitoring*), even with a single SE [15]. In addition to this, the considered SE's have no electronics on board, and the wires of the SE are protected from the environment by a plastic jacket, thus ensuring a lasting service life. Also, it is important to point out that the embedded SEs may also be used for monitoring moisture content during the hydration process of fresh mixture (*ex-ante monitoring*), which can be useful, for example, for verifying that the optimal moisture conditions for the mixture to develop the desired strength properties are achieved.

As for the second application context, i.e. monitoring soil moisture content for optimizing the use of water in agriculture, the basic idea is to bury the SE's in correspondence of cultivations and performing TDR measurements for retrieving the actual water content profile of the soil all along the cultivations. In this way, it would be possible to identify the portion of cultivations that are in need of water, and irrigation could be partialized so as to supply water only to the plants that need it. Indeed, TDR is widely used for monitoring soil moisture content [16]; however, traditional TDR probes for soil moisture applications are local probes [17], and the measurement depends on the placement of the TDR probe in the sample [18]. Conversely, thanks to their wire-like configuration, the SE's considered herein could provide comprehensive information on larger areas.

On the bases of the aforementioned considerations, in this work, several experiments were performed to test the practical feasibility of the proposed sensing systems for the considered applications. In particular, in the first set of experiments, a SE was embedded in a concrete sample, and TDR measurements were performed to monitor the hydration process of the sample. Successively, after the hydration was virtually complete, the sample was subjected to rising damp, and the TDR response was observed as the infiltration of water proceeded.

In the second set of experiments, the proposed TDR-based sensing system was employed to monitor soil water content in a setup that mimicked an in-the-field agricultural cultivation.

Finally, in the third set of experiments, in order to practically evaluate the metrological performance of the considered SE's, six different types of SE were used in an experiment related to the localization of moistened areas of soil, and the obtained results were sistematically compared.

2. Theoretical background

TDR has been widely employed for monitoring applications thanks to the achievable measurement accuracy, to the real-time response, to the relatively-low implementation costs and to the possibility of remote control [19]. Additionally, its flexibility (in terms of adaptability to the desired application) has contributed to making TDR an interesting solution for the most diverse applications, such as fault detection on electric wires [20, 21]; qualitative and quantitative control of liquids [22–24]; moisture measurements of soil [25–28] and of porous materials in general [29]; dielectric characterizations of materials [30–33]; structural analysis [34–36]; etc.

In TDR measurements, an electromagnetic (EM) signal (typically, a voltage step signal with very fast rise-time or a pulse signal) is propagated along a SE, inserted in the STBM. Any impedance variation causes the partial

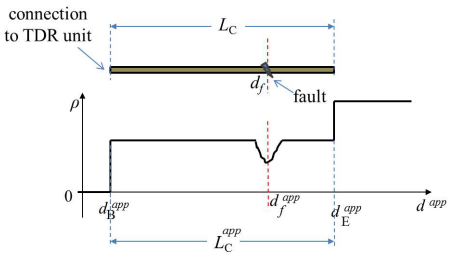

Figure 1. Simplified schematization of a typical TDR reflectogram, where a step-like EM signal propagates along a faulty cable.

reflection of the propagating signal. The reflected signal is acquired by the TDR instrument, and its voltage amplitude is displayed as a function of the travelled electric distance (or apparent distance, d^{app}). The ratio between the amplitude of the reflected signal, v_{refl}, and the amplitude of the generated signal, v_{inc}, gives the value of the reflection coefficient, ρ [37]:

$$\rho = \frac{v_{refl}}{v_{inc}} \tag{1}$$

where $-1 \leq \rho \leq +1$. The direct output of a TDR measurement is a reflectogram, which displays ρ as a function of d^{app}. Through a suitable data processing of the reflectogram (tailored for the specific application), it is possible to retrieve the desired information on the STBM.

For the sake of example, Fig. 1 shows a simplified schematization of a TDR reflectogram for an EM step-like signal propagating through a cable with length L_C in which a fault is present at d_f. The abscissae d_B^{app} and d_E^{app} indicate the typical abrupt changes of ρ in correspondence of the beginning and of the end of the SE, respectively. The quantity d^{app} can be associated to the 'actual' physical length traveled by the signal (d), through the following equation:

$$d^{\text{app}} = \sqrt{\varepsilon_{\text{eff}}}\, d, \tag{2}$$

where ε_{eff} is referred to as effective relative dielectric permittivity of the medium in which the signal propagates [37, 38]. In correspondence of the fault, the ρ exhibits a variation caused by the change of electrical impedance: by analyzing the reflectogram and applying equation (2), it is possible to evaluate the physical position of the fault [19]. Similarly, it is possible to localize other kinds of defects along the profile, including for example infiltration of water. For example, with reference to the example depicted in Fig. 1, the position of the defect may be calculated as follows:

$$d_{\text{eval,f}} = \frac{d_f^{\text{app}} - d_B^{\text{app}}}{L_c^{\text{app}}/L_c}. \tag{3}$$

(a)

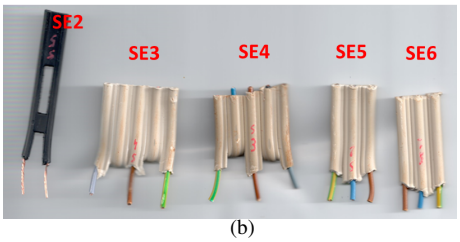

(b)

Figure 2. Picture of portions of SE1 (a) and of SE2, SE3, SE4, SE5 and SE6 (b).

3. Materials and Methods

3.1. Description of the configuration of the used SE's

The experiments on the concrete sample and on the soil were performed using a flexible two-wire sensing element (SE1), similar to the one used in [7] for water leak detection. SE1 consisted of two parallel copper wires (each with cross-section area of 1 mm^2), insulated from each other by a semi-rigid PVC jacket, as shown in Fig. 2(a).

As for the assessment of the performance of the TDR-based sensing system when used in conjunction with different types of SE's, six different configurations of wire-like SE (SE1 and SE2, ..., SE6, as shown in Fig. 2(b)) were comparatively employed for the localization of moistened portions of soil. Similarly to SE1, the SE2 consisted of two metallic wires separated by a plastic jacket; however, in SE2, the mutual distance between the wires was higher, due to the presence of semi-rigid plastic insertions. As for the other SE's, they consisted of three mutually-isolated wires, differing in the mutual distance between the wires.

All the TDR measurements reported in this work were performed through the HyperLabs HL1500 unit:

Figure 3. Preparation of the concrete sample, with the embedding of SE1.

a portable reflectometer that generates a step-like voltage signal with a rise time of approximately 200 ps. The HL1500 has a BNC-type output connector with a 50 Ω electric impedance.
The SE's were connected to the output port of the HL1500 through a short portion of 50-Ω coaxial cable. For the two-wire SE's (i.e. SE1 and SE2), one wire was connected to the central conductor of the coaxial cable, whereas the other was connected to the outer conductor. As for the three-wire SE's (i.e. SE3, SE4, SE5 and SE6), the wires were connected to the coaxial cable in a ground-source-ground fashion, thus resembling a three-rod probe configuration [39].

3.2. Setup for the TDR measurements on concrete-based structures

A concrete sample (with dimensions 100 cm x 10 cm x 8 cm) was prepared and equipped with a sensing element (type SE1), as shown in Fig. 2(a). The letters *B* and *E* indicate the beginning and the end of the SE, respectively. The physical length of the SE was L_{SE} = 98 cm. The concrete mixture was obtained by mixing 6.4 kg of cement, 6.0 kg of water, 16.0 kg of sand, 8.0 kg of gravel, and 10.5 kg of fine gravel. As will be detailed later in this paper, two types of observation were carried out on this sample. First, the hydration process was observed for 28 days through TDR measurements: this allowed to analyze the relation between the change in the TDR response and the advance of the hydration process, thus realizing an *ex-ante monitoring* of the considered structure.
Secondly, after drying, the sample was placed in contact with moistened sand, thus favoring the rising damp phenomenon: also in this case, the relation between the change in the TDR response with the rising damp was observed. This experiment was intended to validate the proposed system for *ex-post monitoring* of building structures, i.e. for possible use in monitoring the infiltration of water in buildings while the structures are in use.

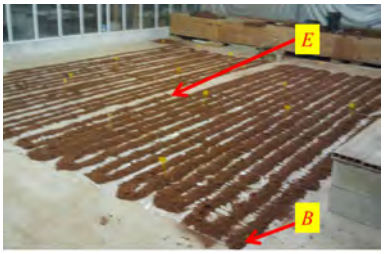

(a)

(b)

Figure 4. Picture of the experimental setup (a) and zoom of the beginning of the SE (b).

3.3. Setup for the experiments related to diffused soil moisture measurements

To assess the applicability of the proposed system for optimization of irrigation in agriculture and to mimic a realistic in-the-field condition, a 90 m-long SE1 was positioned following a serpentine-shaped path, and was covered with soil as shown in Fig. 4 (the serpentine path was chosen so as to fully exploit all the available room). Also in this case, the letters *B* and *E* indicate the beginning and the end of the SE, respectively. Fig. 4(b) shows a zoom in correspondence of the beginning of the SE (a portion of the coaxial cable for the connection to the TDR instrument is also visible).
As detailed later in this paper, starting from the end of the SE, the soil was progressively moistened and the corresponding TDR waveforms were acquired.

3.4. *Test-bed for the characterization of different configurations of SE*

To test the influence of the SE configuration on the performance of the proposed TDR-based sensing system, six types of SE's were cut at a length of 11 m, and were covered with soil. Successively, the soil was moistened in correspondence of different portions (P1, P2, and P3). As schematized in Fig. 5(a), first, the soil was moistened in correspondence of P1. (Subsequently, the soil was moistened also in P2 (Fig. 5(b)); and, finally, it was moistened in P3 (Fig. 5(c)). Fig. 5 shows the distance of P1, P2, and P3 from the beginnings of the SE's. In the figure, the shaded areas indicate the portion of the moistened soil (each extended for approximately 60 cm around the points P1, P2, and P3).
To compare the performance of the SE's in localizing the points of wet soil, the positions of P1, P2 and P3 were considered as unknown and were evaluated through TDR measurements.

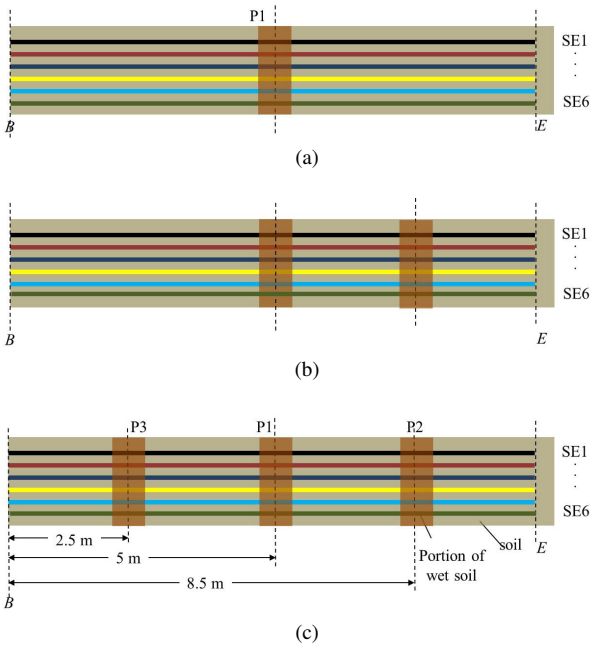

Figure 5. Schematization of the disposition of the six SE's covered with soil, in presence of P1 (a); P1 and P2 (b); P1, P2, and P3 (c).

4. Experimental results

4.1. *Experimental results for monitoring concrete structures*

During the 28-day hydration period, TDR measurements were performed and the variation of the overall effective dielectric constant ($\varepsilon_{\mathrm{eff,con}}$) of the sample was observed. In particular, the value of $\varepsilon_{\mathrm{eff,con}}$ was calculated by applying equation (2) as follows:

$$\varepsilon_{\mathrm{eff,con}} = (L^{\mathrm{app}}_{\mathrm{SE,n}}/L_{\mathrm{SE}})^2 \tag{4}$$

where $L^{\mathrm{app}}_{\mathrm{SE,n}}$ was the apparent length of the SE as calculated from the reflectogram acquired on the n$^{\mathrm{th}}$ day, whereas L_{SE} was the physical length of the SE (in this case, 98 cm).

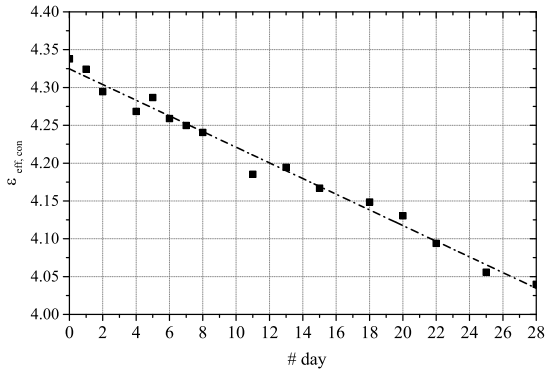

Figure 6. Variation of $\varepsilon_{\mathrm{eff,con}}$ as a function of time.

Fig. 6 shows the variation of $\varepsilon_{\mathrm{eff,con}}$ as a function of the day of observation (each square marker refers to a TDR acquisition performed on that day). It can be seen that there is an almost-linear variation; in fact, the points were linearly fitted and the resulting adjusted R-square was 0.98. In particular, it can be observed that, as the hydration proceeded, the $\varepsilon_{\mathrm{eff,con}}$ decreased as a result of the decrease of free water. In fact, the relative dielectric permittivity of water is approximately 78, whereas af-ter the stoichiometric water has reacted and the excess water evaporated, the resulting concrete has a relative dielectric permittivity in the order of 4-5. In practical applications, once the calibration curve (similar to the one in Fig. 6 has been established for a specific type of SE and for a specific length, the curve can be used to verify the correct advancement of the hydration process.

The second part of the experiment was dedicated to assess the possibility of employing the proposed system also for *ex-post* monitoring of building structures. To this purpose, once the sample had dried up, it was placed in contact with moistened sand (Fig. 7), thus favoring the rising damp. From Fig. 7, it can be seen that the lower portion of the sample appears moistened due to the infiltration of water; the height reached by the infiltrated water is indicated as h_{r}.

Figure 7. Picture of the experimental setup for monitoring the rising-damp.

While the rising damp proceeded, the TDR reflectograms were acquired. Fig. 8 shows the acquired reflectograms in a 7-day period. It can be seen that, as h_r increased, also the apparent length of the SE increased. In addition to this, as a result of the increase of water content at the base of the sample, in correspondence of the end of the SE, there is also a decrease of the ρ value.

4.1.1. *Discussions on the use of the proposed system for monitoring building structures*

As well known, it is extremely important to be able to constantly monitor the structures and to promptly inter-

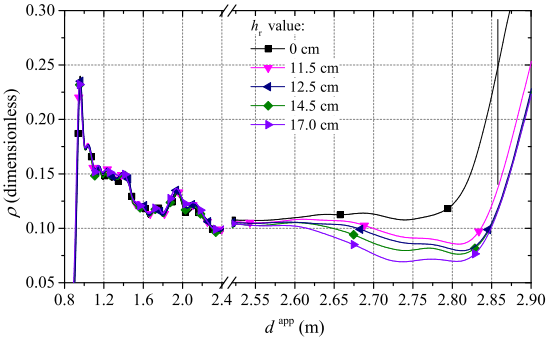

Figure 8. Reflectograms acquired as the infiltration of water proceeded.

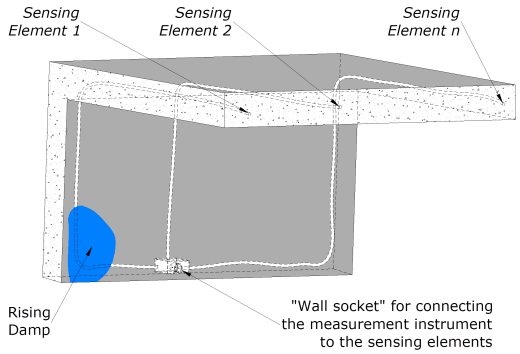

Figure 9. Schematization of the possible implementation of SE's for monitoring building structures.

vene with the necessary maintenance, otherwise moisture/water infiltration may lead to severe deterioration phenomena of building infrastructures.

In practical applications, for example in a building, the connection to the SE (the point indicated as B) could be left accessible simply through a wall socket, thus facilitating the connection to the TDR instrument and speeding-up the analysis. Fig. 9 shows a schematization of a possible practical implementation of the proposed sensing system. Similarly to monitoring in civil buildings, viaducts, bridges and a lot of other infrastructures could benefit from the embedding of these SE's. Additionally, the application of this system is not limited to moisture content profiling; on the contrary, it would also allow to periodically monitor the health status of the structures. The embedded SE's, in fact, could also be used to detect the incipient growth of cracks. For example, by acquiring the TDR response right after a structure has been completed, it would be possible to store it in a data-base and to use it for subsequent comparative purposes when checking for the health status of the structure (ex-post monitoring): any change in the TDR response could be related to possible degradation/aging of the structure.

4.2. *Experimental results for TDR-based diffused soil-moisture measurements in agriculture*

In the conditions depicted in Fig. 4, the soil was moistened 10 m at a time, starting from the end of the SE (point E) up to the beginning (point B); at each moistening step, the corresponding TDR reflectogram was acquired. Fig. 10(a) shows the acquired reflectograms; L_{wet} indicates the total length of the moistened portion of soil. It can be seen that, starting from the dry condition (L_{wet} = 0 m) to the totally-moistened

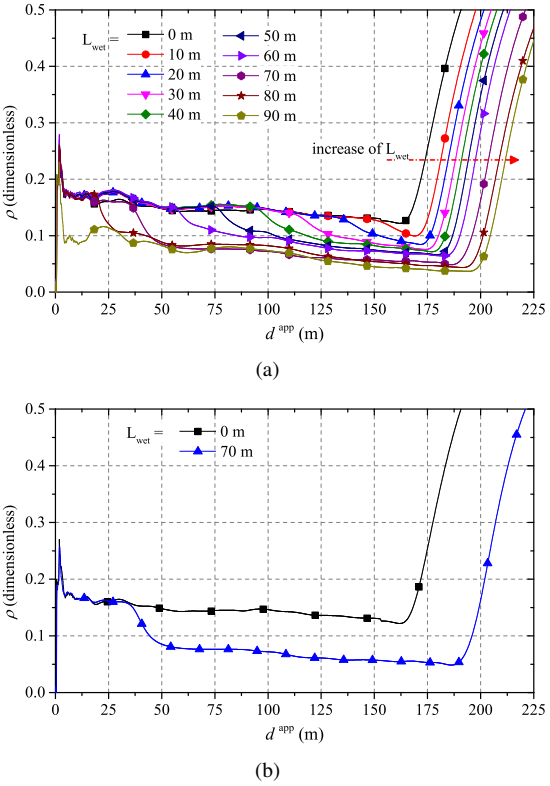

Figure 10. Reflectograms acquired, with the experimental setup shown in Fig. 4, by moistening 10 m of soil at a time, starting from the end of the buried SE (a). Comparison of two reflectograms (b).

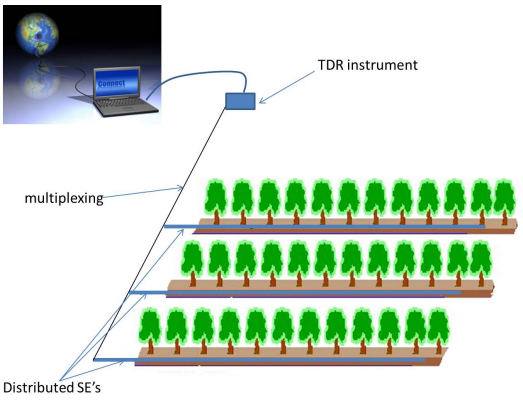

Figure 11. Schematization of the possible configuration of a network of diffused SE's for optimization of irrigation in agriculture.

condition (L_{wet} = 90 m), the apparent length of the SE increased. In particular, as a result of the increase of the ε_{eff} value of the portion of moistened soil, the abscissa of the end of the SE shifts towards higher apparent distances. For the sake of clarity, Fig. 10(b) shows the comparison between the reflectogram acquired for L_{wet} = 0 m and the reflectogram for L_{wet} = 70 m. The obtained results show that, even in long distances and even in presence of turns, one single SE can allow to obtain comprehensive information on a large area, easily discriminating between wet and dry portions of soil.

4.2.1. Discussions on the use of the proposed method for irrigation management in agriculture

In practical applications, such diffused monitoring system could be used not only to monitor the soil wa-ter content of cultivations, but also to localize possible portions of the cultivation affected by water shortage. In fact, through specific calibration curves, it would be possible to associate the apparent distance as calculated from the reflectogram, to the actual position of the portion of soil in need of water. The TDR-based monitoring system could be integrated with the irrigators; therefore, when the measured soil water content falls below (or ex-ceeds) a pre-established threshold, the monitoring sys-tem will activate (or deactivate) the irrigation system, completely or partially.

For the sake of example, Fig. 11 shows the schematization of a possible application of a TDR-based system for monitoring irrigation in agriculture: each diffused SE monitors the water content of an entire row of trees (rather than having a punctual sensing element at the roots of each tree) and a multiplexing unit allows conrolling a multitude of SE's through a single TDR in-

strument.

5. Experimental assessment of the performance of different biwires

In order to assess the proposed monitoring system from a metrological point of view, in this experiment, six different types of SE were covered with soil and their TDR response, with varying moisture conditions, was observed. First, while the soil was still dry, a reflectogram was acquired through each of the SE: the obtained reflectograms are shown in Fig. 12(a). It can be seen that, overall, in the dry condition, all the reflectograms are practically horizontal in correspondence of the sensing element (except for the effect of the transition coaxial/multiwire, which causes a small change in correspondence of $d^{app} = 7$ m). Clearly, each type of SE exhibits a different behavior, due to the different characteristic electrical impedance. In particular, it can be seen that SE3 and SE4 have a similar behavior. Also, SE5 and SE6's behavior is similar; although the corresponding reflection coefficient is higher than that of SE3 and SE4 (as a result of the higher electrical impedance). SE2 has a higher reflection coefficient and a shorter apparent length; this is probably a result of the higher distance between the two metallic wires. Finally, SE1 behaves similarly to the previous experiments; and its characteristic electrical impedance is the lowest among the considered SE's.

Successively, the soil was moistened in correspondence of P1 (as depicted in Fig. 5(a)), and the corresponding reflectograms were acquired; the results are shown in Fig. 12(b). It can be seen that a local minimum (due to the presence of P1) has appeared between $d^{app} = 12.5$ m and $d^{app} = 16.0$ m.

Similarly, Fig. 12(c) and Fig. 12(d) show the reflectograms acquired in correspondence of the conditions depicted in Fig. 5(b), and Fig. 5(c), respectively.
It can be seen that, as the number of moistened portions of soil increased, the number of minima in reflectograms increased. From each reflectogram, the position of the moistened portions of soil was evaluated through the leak-localization procedure reported in [40]. For example, considering SE1, from the reflectogram in Fig. 12(b), the position of P1 was calculated as

$$L_{\mathrm{eval,P1}} = \frac{L^{\mathrm{app}}_{\mathrm{min}}}{L^{\mathrm{app}}_{\mathrm{SE}}/L_{\mathrm{SE}}}, \tag{5}$$

where $L^{\mathrm{app}}_{\mathrm{min}} = d^{\mathrm{app}}_{\mathrm{min}} - L^{\mathrm{app}}_{\mathrm{B}}$ and $L^{\mathrm{app}}_{\mathrm{SE}} = L^{\mathrm{app}}_{\mathrm{E}} - L^{\mathrm{app}}_{\mathrm{B}}$. The quantity $d^{\mathrm{app}}_{\mathrm{min}}$ is the abscissa of the local minimum.

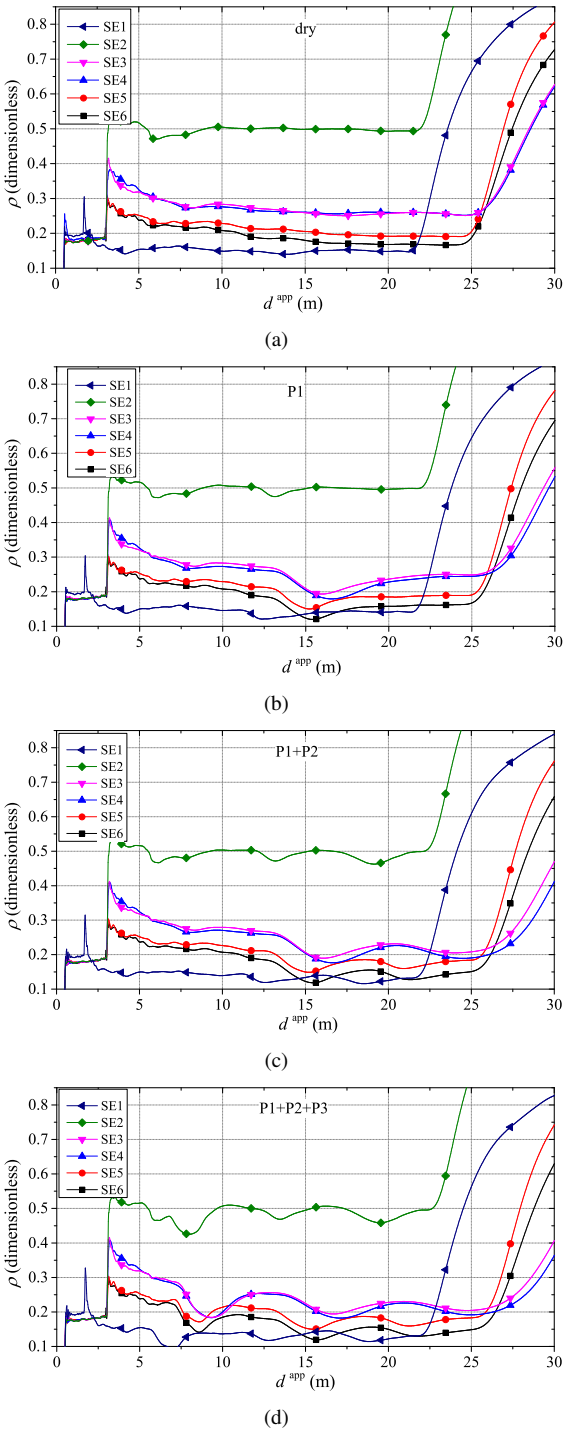

Figure 12. Reflectograms acquired, through the six SE's, with dry soil (a); in presence of P1 (b); in presence of P1 and P2 (c); and in presence of P1, P2 and P3 (d).

Table 1. Summarized data related to the evaluation of the positions of P1, P2 and P3 through the different SE's. The corresponding percentage error values are also reported

	$L_{eval,P1}$ (m)	$\lvert\%e_{P1}\rvert$	$L_{eval,P2}$ (m)	$\lvert\%e_{P2}\rvert$	$L_{eval,P3}$ (m)	$\lvert\%e_{P3}\rvert$
SE1	5.62	2.2	-	-	-	-
	5.75	4.5	8.88	4.5		-
	5.84	6.2	9.03	6.2	2.82	12.8
SE2	5.57	1.3	-	-		-
	5.60	1.8	8.90	4.7		-
	5.74	4.4	9.09	6.9	2.81	12.4
SE3	5.77	4.9	-	-		-
	5.81	5.6	9.34	9.9		-
	6.07	10.3	9.74	14.6	2.80	12.0
SE4	5.99	8.9	-	-	-	-
	6.02	9.5	6.41	24.6	-	
	6.23	13.3	9.71	14.2	2.78	11.2
SE5	5.74	4.4	-	-	-	-
	5.73	4.2	8.43	0.8	-	-
	5.85	6.4	8.59	1.1	2.61	4.4
SE6	5.80	5.5	-	-	-	-
	5.82	5.8	8.56	0.7	-	-
	5.94	8.0	8.78	3.3	2.59	3.6

Table 1 summarizes the results related to the evaluation of the position of P1, P2 and P3. Table 1 also reports the percentage error values ($\%e_{P1}$, $\%e_{P2}$ and $\%e_{P3}$). For this calculation, the central points of each moistened area were considered as reference 'true' values. The obtained percentage error values are in agreement with the 5% percentage error obtained in [7], when using the SE1 in a similar scenario (i.e. for the evaluation of the position of a leak in an underground pipes through TDR measurements). It should be pointed out that it was decided to use the percentage error as a figure of merit of the performance of the system (rather than evaluating the experimental uncertainty), because in the experiments there are some variables which are difficult to repeat (one being the unpredictable diffusion of water in possible repetitions of P1, P2, and P3).

When only one moistened portion is present (P1), SE1 and SE2 provided the lowest errors. However, when P1, P2, and P3 are simultaneously present, the sensing elements SE5 and SE6 are affected by the lowest error. Probably, the reason is that the configuration of SE5 and SE6 resembles that of a three-rod probe, and the distribution of the EM field is more simmetric. In addition to this, the fact that the wires are closer than in SE3 and SE4, probably leads on one hand to a smaller sensing volume (in the transverse section, but on the other hand allows a better discrimination of moisture differences in areas in close proximity.

Overall, it can be seen that, for each SE, the evaluation of the position of P1, P2 and P3 is affected by a higher error as the number of moistened portions of soil increases. This is due to the fact that, in presence of multiple moistened points, there is a slight overestimation of the involved distances, caused by a slight overestimation in the estimated value of ε_{eff}. Indeed, a more accurate algorithm should consider the variation of the effective dielectric constant every time a new portion of soil is moistened; this will be the subject of further studies; however, for the sake of the purposes of this work, the obtained results confirm the optimal potential of the method. In fact, the evaluation of the positions of the three moistened portions of soil when they are simultaneously present in such a short length (i.e. 11 m) is not a trivial task, and provides indication also of the sensitivity of the method in discriminating closely-spaced moistened portions.

From the operating point of view, the SE1 and SE2 configurations may be more suitable for those applications in which it is expected to have to locate only one transition between moistened area and dry area. For example, in building structures, the rising damp (coming from below) is expected to provoke a single transition between moistened and dry areas. Vice versa, for applications such as water content control in agriculture, in which one may expect to have a more articulated distribution of moistened areas, the SE5 and Se6 configurations may be more suitable.

6. Conclusions

In this work, the possibility of using diffused, flexible, wire-like SE's in conjunction with TDR for diagnostic and monitoring purposes was addressed. In particular, two practical applications contexts were considered, namely monitoring of building structures and monitoring of water irrigation process in agriculture. The experiments carried out for each of these applications confirmed the practical feasibility of the proposed system. Furthermore, in order to test the influence of different SE configurations on the TDR response, an additional experiment was performed to compare the performance of six types of SE.

While additional experiments are to be carried out in order to fully test and characterize the proposed system for the intended purposes, the ultimate challenge, in the long-term, will be to realize a comprehensive monitoring platform, based on 'sensing elements networks' that could possibly be interfaced with a common (single) technological infrastructure and that could be simply controlled through smartphone or computer-based applications.

Acknowledgments

The work related to the monitoring of building structure was carried out within the Technology Transfer Programme 'An Innovative Diffused Monitoring of Moisture and Health in Building Structures', and has received funding from the European Unions 7th Framework Programme for research, technological development and demonstration under the TETRACOM grant agreement no. 609491.

References

[1] A. Calia, M. Lettieri, G. Leucci, L. Matera, R. Persico, M. Sileo, The mosaic of the crypt of st. Nicholas in Bari (Italy): Integrated gpr and laboratory diagnostic study, Journal of Archaeological Science 40 (12) (2013) 4162–4169.

[2] F. Gabellone, G. Leucci, N. Masini, R. Persico, G. Quarta, F. Grasso, Non-destructive prospecting and virtual reconstruction of the chapel of the Holy Spirit in Lecce, italy, Near Surface Geophysics 11 (2) (2013) 231–238.

[3] M. Solla, H. González-Jorge, H. Lorenzo, P. Arias, Uncertainty evaluation of the 1 GHz GPR antenna for the estimation of concrete asphalt thickness, Measurement 46 (9) (2013) 3032–3040.

[4] M. Kempin, M. Ghasr, J. Case, R. Zoughi, Modified waveguide flange for evaluation of stratified composites, IEEE Transactions on Instrumentation and Measurement 63 (6) (2014) 1524–1534.

[5] S. Kharkovsky, R. Zoughi, Microwave and millimeter wave nondestructive testing and evaluation - overview and recent advances, IEEE Instrumentation Measurement Magazine 10 (2) (2007) 26–38.

[6] A. Cataldo, G. Cannazza, E. De Benedetto, N. Giaquinto, A new method for detecting leaks in underground water pipelines, IEEE Sensors Journal 12 (6) (2012) 1660–1667.

[7] A. Cataldo, G. Cannazza, E. De Benedetto, N. Giaquinto, A TDR-based system for the localization of leaks in newly installed, underground pipes made of any material, Measurement Science and Technology 23 (10), p. 105010.

[8] A. Cataldo, E. De Benedetto, G. Cannazza, N. Giaquinto, M. Savino, F. Adamo, Leak detection through microwave reflectometry: From laboratory to practical implementation, Measurement 47 (2014) 963–970.

[9] L. Alwis, T. Sun, K. Grattan, Optical fibre-based sensor technology for humidity and moisture measurement: Review of recent progress, Measurement 46 (10) (2013) 4052 – 4074.

[10] C. Sayde, C. Gregory, M. Gil-Rodriguez, N. Tufillaro, S. Tyler, N. van de Giesen, M. English, R. Cuenca, J. S. Selker, Feasibility of soil moisture monitoring with heated fiber optics, Water Resources Research 46 (6) (2010) n/a–n/a.

[11] M. Alam, R. Bhuiyan, R. Dougal, M. Ali, Concrete moisture content measurement using interdigitated near-field sensors, IEEE Sensors Journal 10 (7) (2010) 1243–1248.

[12] A. Norris, M. Saafi, P. Romine, Temperature and moisture monitoring in concrete structures using embedded nanotechnology/microelectromechanical systems (MEMS) sensors, Construction and Building Materials 22 (2) (2008) 111–120.

[13] P. Pursula, I. Marttila, K. Nummila, H. Seppa, High frequency and ultrahigh frequency radio frequency identification passive sensor transponders for humidity and temperature measurement within building structures, IEEE Transactions on Instrumentation and Measurement 62 (9) (2013) 2559–2566.

[14] J. Ong, Z. You, J. Mills-Beale, E. L. Tan, B. Pereles, K. G. Ong, A wireless, passive embedded sensor for real-time monitoring of water content in civil engineering materials, IEEE Sensors Journal 8 (12) (2008) 2053–2058.

[15] A. Cataldo, E. De Benedetto, G. Cannazza, Hydration monitoring and moisture control of cement-based samples through embedded wire-like sensing elements, IEEE Sensors Journal 15 (2) (2014) 1208–1215.

[16] S. L. S.U., D. Singh, M. S. Baghini, A critical review of soil moisture measurement, Measurement 54 (2014) 92–105.

[17] P. A. Ferre, J. H. Knight, D. L. Rudolph, R. G. Kachanoski, A numerically based analysis of the sensitivity of conventional and alternative time domain reflectometry probes, Water Resour. Res. 36 (9) (2000) 2461–2468.

[18] T. Pastuszka, J. Krzyszczak, C. SÅawiÅski, K. Lamorski, Effect of time-domain reflectometry probe location on soil moisture measurement during wetting and drying processes, Measurement 49 (2014) 182–186.

[19] A. Cataldo, E. De Benedetto, Broadband reflectometry for diagnostics and monitoring applications, IEEE Sensors Journal 11 (2) (2011) 451–459.

[20] D. AgreÅ, Cable-fault location using regression functions applied to a reflectogram, Measurement 30 (2) (2001) 85–93.

[21] L. Bo, C. Peng, X. Liu, A novel redundant haar lifting wavelet analysis based fault detection and location technique for telephone transmission lines, Measurement 51 (2014) 42–52.

[22] E. Piuzzi, A. Cataldo, L. Catarinucci, Enhanced reflectometry measurements of permittivities and levels in layered petrochemical liquids using an in-situ coaxial probe, Measurement 42 (5) (2009) 685 – 696.

[23] E. Piuzzi, C. Merla, G. Cannazza, A. Zambotti, F. Apollonio, A. Cataldo, P. D'Atanasio, E. De Benedetto, M. Liberti, A comparative analysis between customized and commercial systems for complex permittivity measurements on liquid samples at microwave frequencies, IEEE Transactions on Instrumentation and Measurement 62 (5) (2013) 1034–1046.

[24] A. Cataldo, E. Piuzzi, G. Cannazza, E. De Benedetto, L. Tarricone, Quality and anti-adulteration control of vegetable oils through microwave dielectric spectroscopy, Measurement 43 (8) (2010) 1031 – 1039.

[25] K. M. O'Connor, C. H. Dowding, GeoMeasurements by Pulsing TDR Cables and Probes, CRC Press, UK, 1999.

[26] G. C. Topp, J. L. Davis, A. P. Annan, Electromagnetic determination of soil water content: measurements in coaxial transmission lines, Water Resources Research 16 (1980) 574–582.

[27] T. J. Heimovaara, A. G. Focke, W. Bouten, J. M. Verstraten, Assessing temporal variation in soil water composition with time domain reflectometry, Soil Science Society of America Journal 59 (1995) 689–698.

[28] K. Noborio, Measurement of soil water content and electrical conductivity by time domain reflectometry: a review, Computers and Electronics in Agriculture 31 (3) (2001) 213–237.

[29] R. Cerny, Time-domain reflectometry method and its application for measuring moisture content in porous materials: a review, Measurement 42 (3) (2009) 329–336.

[30] P. Sorichetti, C. Matteo, Low-frequency dielectric measurements of complex fluids using high-frequency coaxial sample cells, Measurement 40 (4) (2007) 437–449.

[31] P. M. Kumar, M. Malathi, Dielectric relaxation studies of nylon-11 with phenol derivatives in non-polar solvents using time do-

main reflectometry, Journal of Molecular Liquids 145 (2009) 5–7.

[32] R. Nozaki, T. K. Bose, Broadband complex permittivity measurements by time-domain spectroscopy, IEEE Transactions on Instrumentation and Measurement 39 (6) (1990) 945–951.

[33] N. Miura, S. Yagihara, S. Mashimo, Microwave dielectric properties of solid and liquid foods investigated by time-domain reflectometry, Journal of Food Science 68 (4) (2003) 1396–1403.

[34] J. Bishop, D. Pommerenke, G. Chen, A rapid-acquisition electrical time-domain reflectometer for dynamic structure analysis, IEEE Transactions on Instrumentation and Measurement 60 (2) (2011) 655–661.

[35] C. Furse, P. Smith, M. Diamond, Feasibility of reflectometry for nondestructive evaluation of prestressed concrete anchors, IEEE Sensors Journal 9 (11) (2009) 1322–1329.

[36] S. Sun, D. Pommerenke, J. Drewniak, G. Chen, L. Xue, M. Brower, M. Koledintseva, A novel TDR-based coaxial cable sensor for crack/strain sensing in reinforced concrete structures, IEEE Transactions on Instrumentation and Measurement 58 (8) (2009) 2714–2725.

[37] J. R. Andrews, Time Domain Reflectometry (TDR) and Time Domain Transmission (TDT) Measurement Fundamentals, Boulder, CO: Picosecond Pulse Labs, 2004, Application Note AN-15.

[38] Time Domain Reflectometry Theory, Palo Alto, CA, Agilent Application Note 1304-2 (May 2006).

[39] A. Cataldo, G. Cannazza, E. De Benedetto, L. Tarricone, M. Cipressa, Metrological assessment of TDR performance for moisture evaluation in granular materials, Measurement 42 (2) (2009) 254 – 263.

[40] A. Cataldo, G. Cannazza, E. De Benedetto, N. Giaquinto, A TDR-based system for the localization of leaks in newly installed, underground pipes made of any material, Measurement Science and Technology 23 (10), p. 105010.